Carbene Formation in the Reactions of $LFe\{(CH_2)_3Br\}(CO)_2$ (L = Cp, Cp*) with I^-. X-ray Crystal Structures of $CpFeI(CO)\{=\overline{C(CH_2)_3O}\}$ and $CpFeI(CO)\{=\overline{CCMe_2(CH_2)_2O}\}$. Analysis of the Carbene Orientations

Harry Adams, Neil A. Bailey, Martin Grayson, Christopher Ridgway, Arnold J. Smith, Paul Taylor, and Mark J. Winter*

Department of Chemistry, The University, Sheffield S3 7HF, England

Catherine E. Housecroft

University Chemistry Laboratory, University of Cambridge, Lensfield Road, Cambridge CB2 1EW, England

Received December 29, 1989

The reaction of $LFe\{(CH_2)_3Br\}(CO)_2$ (L = Cp, Cp*) with LiI affords the new carbene complexes $LFeI(CO)\{=\overline{C(CH_2)_3O}\}$, both of which have been characterized spectroscopically; the Cp species has been characterized by X-ray crystallography as well. The unusual feature of the structure of $CpFeI(CO)\{=\overline{C(CH_2)_3O}\}$ is the presence of two conformers within the unit cell. To a first approximation these are related by a rotation about the Fe=C axis. The reasons for the presence of the two conformers are examined by molecular mechanics and Fenske-Hall type calculations. Treatment of $CpFeI(CO)\{=\overline{C(CH_2)_3O}\}$ with LDA followed by MeI results in $CpFeI(CO)\{=\overline{CCMe_2(CH_2)_2O}\}$, whose crystal structure has just the single conformer in the unit cell.

Migrations of groups such as hydride[1] and alkyl[2] to carbene are important in that they represent the formation of new C-H or C-C bonds and such migrations are fundamental steps within organometallic chemistry. These migrations are frequently postulated in reaction mechanisms but not so frequently directly observed. Our interest in this area was kindled by our observation[3] that the hydride ligand of $CpMoH(CO)_2\{=\overline{C(CH_2)_3NMe}\}$ (Cp = η^5-C_5H_5) undergoes migration to the cyclic carbene ligand. Since then we have explored various migrations to carbene involving molybdenum and tungsten complexes.[4] The required precursor species for these studies are complexes of the general formula L_nMH(carbene). They are made by reduction of the complexes L_nMI(carbene)[5] with Na-$C_{10}H_8$ to form the anions $[L_nM(carbene)]^-$ followed by protonation of such anions to form the required hydridometal carbene complexes L_nMH(carbene). In this paper, we explore the synthesis of some iron carbene complexes L_nFeI(carbene) that might be suitable precursors for ligand to carbene migrations and discuss some unusual features of these compounds.

Scheme I

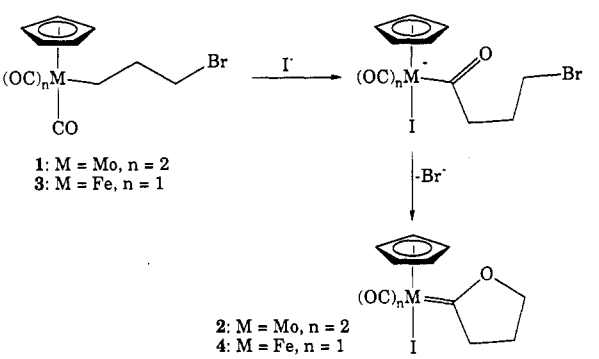

Results and Discussion

$CpFeI(CO)\{=\overline{C(CH_2)_3O}\}$ (4). The reactions of bromoalkyl complexes $LM\{(CH_2)_3Br\}(CO)_3$ (M = Mo, W; L = Cp, Cp' (η^5-C_5H_4Me), Cp* (η^5-C_5Me_5), (etc.) with iodide are efficient syntheses of the carbene complexes $LMI(CO)_2\{=\overline{C(CH_2)_3O}\}$.[6] The mechanism of carbene forma-

(1) (a) Shapley, J. R.; Calvert, R. V. *J. Am. Chem. Soc.* **1977**, *99*, 5225. (b) Empsall, H. D.; Hyde, E. M.; Markham, R.; McDonald, W. S.; Norton, M. C.; Shaw, B. L.; Week, B. *J. Chem. Soc., Chem. Commun.* **1979**, 498. (c) Threlkel, R. S.; Bercaw, J. E. *J. Am. Chem. Soc.* **1981**, *103*, 2650. (d) Clark, G. R.; Headford, C. E. L.; Marsden, K.; Roper, W. R. *J. Organomet. Chem.* **1982**, *231*, 335. (e) Thorn, D. L.; Tulip, T. H. *Organometallics* **1982**, *1*, 1580. (f) Van Asselt, A.; Burger, B. J.; Gibson, V. C.; Bercaw, J. E. *J. Am. Chem. Soc.* **1986**, *108*, 5347. (g) Turner, H. W.; Schrock, R. R.; Fellmann, J. D.; Holmes, S. J. *J. Am. Chem. Soc.* **1983**, *105*, 4942. (h) Barger, P. T.; Bercaw, J. E. *Organometallics* **1984**, *3*, 278. (i) Green, J. C.; Green, M. L. H.; Morley, C. P. *Organometallics* **1985**, *4*, 1302. (j) Werner, H.; Roder, K. *J. Organomet. Chem.* **1986**, *310*, C51. (k) Le Bozec, H.; Fillaut, J.-L.; Dixneuf, P. H. *J. Chem. Soc., Chem. Commun.* **1986**, 1182. (l) Parkin, G.; Bunel, E.; Burger, B. J.; Trimmer, M. S.; Van Asselt, A.; Bercaw, J. E. *J. Mol. Catal.* **1987**, *41*, 21. (m) Collman, J. P.; Hegedus, L. S.; Norton, J. R.; Finke, R. G. In *Pinciples and Applications of Organotransition Metal Chemistry*, 2nd ed.; University Science Books: Mill Valley, CA, 1987; pp 379-382.

(2) (a) Cooper, N. J.; Green, M. L. H. *J. Chem. Soc., Chem. Commun.* **1974**, 209. (b) Schrock, R. R. *J. Am. Chem. Soc.* **1974**, *96*, 6796. (c) Cooper, N. J.; Green, M. L. H. *J. Chem. Soc., Dalton Trans.* **1979**, 1121. (d) Schrock, R. R. *Acc. Chem. Res.* **1979**, *12*, 98. (f) Dawoodi, A.; Green, M. L. H.; Mtetwa, V. S. B.; Prout, K. J. *J. Chem. Soc., Chem. Commun.* **1982**, 1410. (e) Canestrari, M.; Green, M. L. H. *J. Chem. Soc., Dalton Trans.* **1982**, 1789. (f) Mahmoud, K. A.; Rest, A. J.; Alt, H. G. *J. Chem. Soc., Chem. Commun.* **1983**, 1011. (g) Brookhart, H.; Green, M. L. H. *J. Organomet. Chem.* **1983**, *250*, 395. (h) Cross, R. J. In *The Chemistry of the Metal-Carbon Bond*; Hartley, F. R., Patai, S., Eds.; Wiley: New York, 1985; Vol. 2, Chapter 8. (i) Yang, G. K.; Peters, K. S.; Vaida, V. *J. Am. Chem. Soc.* **1986**, *108*, 2511.

(3) (a) Osborn, V. A.; Parker, C. A.; Winter, M. J. *J. Chem. Soc., Chem. Commun.* **1986**, 1185. (b) Davey, C. E.; Devonshire, R.; Winter, M. J. *Polyhedron* **1989**, *8*, 1863. (c) Winter, M. J. *Polyhedron* **1989**, *8*, 1583.

(4) (a) Winter, M. J.; Woodward, S. *J. Chem. Soc., Chem. Commun.* **1989**, 457. (b) Winter, M. J.; Woodward, S. *J. Organomet. Chem.* **1989**, *361*, C18.

(5) Osborn, V. A.; Winter, M. J. *J. Chem. Soc., Chem. Commun.* **1985**, 1744.

0276-7333/90/2309-2621$02.50/0

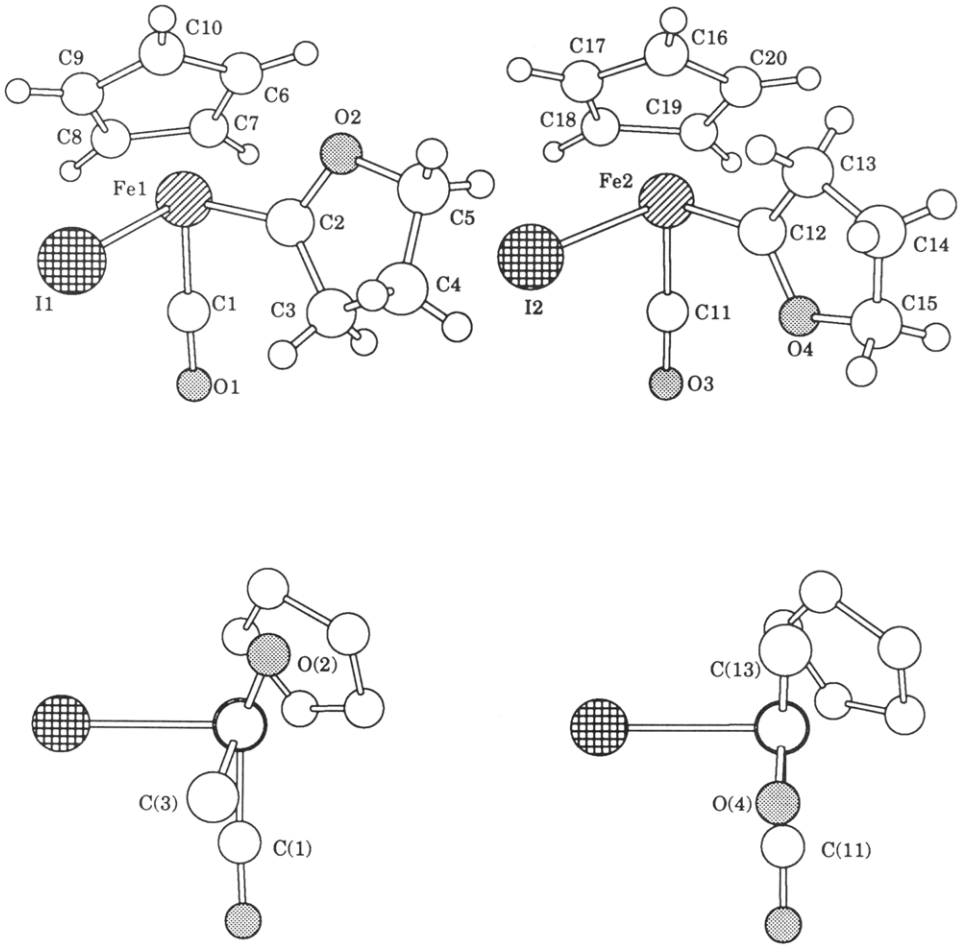

Figure 1. Structures of **4a** (top left) and **4b** (top right) found within the unit cell of CpFeI(CO){=C(CH$_2$)$_3$O} (**4**). The lower diagrams show **4a** (left) and **4b** (right) viewed along the Fe–carbene axis to illustrate the carbene orientations with all hydrogens and C(4), C(5), C(14), and C(15) omitted for clarity.

tion involves attack of iodide on the metal of **1**, for instance. This induces a migratory insertion step as outlined in Scheme I. The resulting anionic acyl species cyclizes while losing Br^-, resulting in the final product **2**.

We reasoned that this approach with incoming iodide should also work for the corresponding iron system **3** to give **4**, provided a number of potential side reactions do not compete too successfully with the mechanism of Scheme I. A modification of this approach works successfully with neutral PPh_3 as incoming ligand, in which case the product is the cation $[CpFe(CO)(PPh_3)\{=\overline{C(CH_2)_3O}\}]^+$.[7]

Complex **3** is formed in the reaction of $[CpFe(CO)_2]^-$ with $Br(CH_2)_3Br$.[8] It is necessary to control the temperature and stoichiometry during its synthesis in order that formation of the dimetallaalkane $Cp(OC)_2Fe(CH_2)_3Fe(CO)_2Cp$ is minimized. Adding LiI to a solution of **3** in THF followed by stirring at ambient temperature for 1 day results in complex **4**, isolated in 49% yield. No intermediates were observed. The side products are minor amounts of $CpFeI(CO)_2$ and $[CpFe(CO)_2]_2$. The spectroscopic data of the major product are in accord with the structure **4**. In particular, a signal at δ 331.0 in the ^{13}C NMR spectrum indicates a carbene. The six protons are manifested as six signals in the ^1H NMR spectrum as a consequence of the chiral iron center. There is no sign of temperature dependence in the ^1H or ^{13}C NMR spectra on cooling as far as −90 °C in toluene-d_8, and so at first sight the X-ray crystal structure of **4** is something of a surprise. It shows two conformers within the unit cell (Figure 1). The failure to observe these conformers by NMR spectroscopy even at low temperatures is a consequence of facile rotation around the Fe=C bond. This conclusion is reinforced by the low barriers to carbene rotation found in the following calculations.

The two conformers consist of essentially identical conventional CpFeI(CO) fragments each bonded to a 2-oxacyclopentylidene ring. The three basal ligands are mutually perpendicular to within 2° (for **4a**) and 3° (for **4b**). The {=C(CH$_2$)$_3$O} group is attached by a short, formal Fe=C bond of length 1.87 Å (**4a**) and 1.86 Å (**4b**). To a first approximation, the two isomers are related by a rotation about the Fe=C axis. In isomer **4b**, the nonhydrogen atoms of the 2-oxacyclopentylidene ring are closely coplanar (rms deviation 0.012 Å) and are also coplanar with the Fe–carbonyl unit. The torsion angle C(12)–Fe(2)–C(11)–O(4) is +3.5°. The sense of the oxygen

(6) (a) Bailey, N. A.; Chell, P. L.; Mukhopadhyay, A.; Tabbron, H. E.; Winter, M. J. *J. Chem. Soc., Chem. Commun.* **1982**, 215. (b) Bailey, N. A.; Chell, P. L.; Manuel, C. P.; Mukhopadhyay, A.; Rogers, D.; Tabbron, H. E.; Winter, M. J. *J. Chem. Soc., Dalton Trans.* **1983**, 2397. (c) Adams, H.; Bailey, N. A.; Osborn, V. A.; Winter, M. J. *J. Organomet. Chem.* **1984**, *284*, C1. (d) Osborn, V. A.; Winter, M. J. *Polyhedron* **1986**, *5*, 435. (e) Adams, H.; Bailey, N. A.; Osborn, V. A.; Winter, M. J. *J. Chem. Soc., Dalton Trans.* **1986**, 2127. (f) Bailey, N. A.; Dunn, D. A.; Foxcroft, C. N.; Harrison, G. R.; Winter, M. J.; Woodward, S. *J. Chem. Soc., Dalton Trans.* **1988**, 1449.

(7) Moss, J. R. *J. Organomet. Chem.* **1982**, *231*, 229.

(8) (a) King, R. B. *Inorg. Chem.* **1963**, *2*, 531. (b) Pope, L.; Sommerville, P.; Laing, M.; Hindson, K. J.; Moss, J. R. *J. Organomet. Chem.* **1976**, *112*, 309.

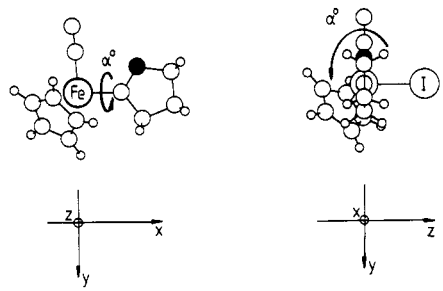

Figure 2. Axes definitions for the MM2 and Fenske–Hall calculations.

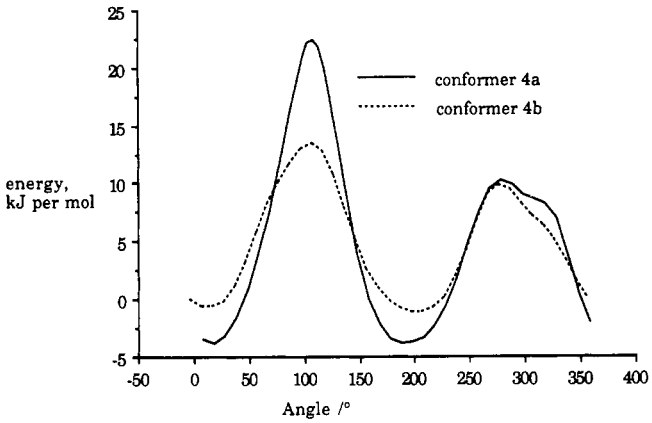

Figure 3. Energy of rotation according to MM2 calculations for **4a** and **4b**. In each case, the 0° point corresponds to the orientation at which the C(carbonyl)–Fe–C(carbene)–O dihedral angle is zero.

atom is anti with respect to the cyclopentadienyl ring and syn to the carbonyl. The sense of the oxygen atom in the other conformer **4a** is such that it lies syn with respect to the cyclopentadienyl ring and anti to the carbonyl. In this case, the 2-oxacyclopentylidene ring is less planar (rms deviation 0.12 Å) and is not coplanar with the Fe–carbonyl unit. When it is viewed along the iron–carbene vector, the ring is seen to lie between the carbonyl and iodide groups. The torsion angle C(1)–Fe(1)–C(2)–O(2) is −158.5°. One of the carbon atoms, C(4), lies off the plane of the 2-oxacyclopentylidene ring so that the ring has an overall envelope conformation.

Why are these isomers present in the unit cell? We examined this problem using a simple molecular mechanics approach[9] (MM2) to probe steric interactions and by Fenske–Hall type calculations[10] to probe for electronic factors.

Molecular Mechanics Calculations. Single-geometry calculations were performed with use of the crystal coordinates of both molecules for the energies associated with a series of orientations generated by rotating the carbene group clockwise as viewed from the iron to the carbene down the Fe=C bond (see Figure 2 for the axis system). No flexibility was therefore given to the carbene ring or to the CpFe unit. No attempt was made to examine intermolecular effects.

The results for the two orientations are superimposed in Figure 3. The Fe–C(carbonyl) unit is used as reference, with the angle 0° representing the orientation of each

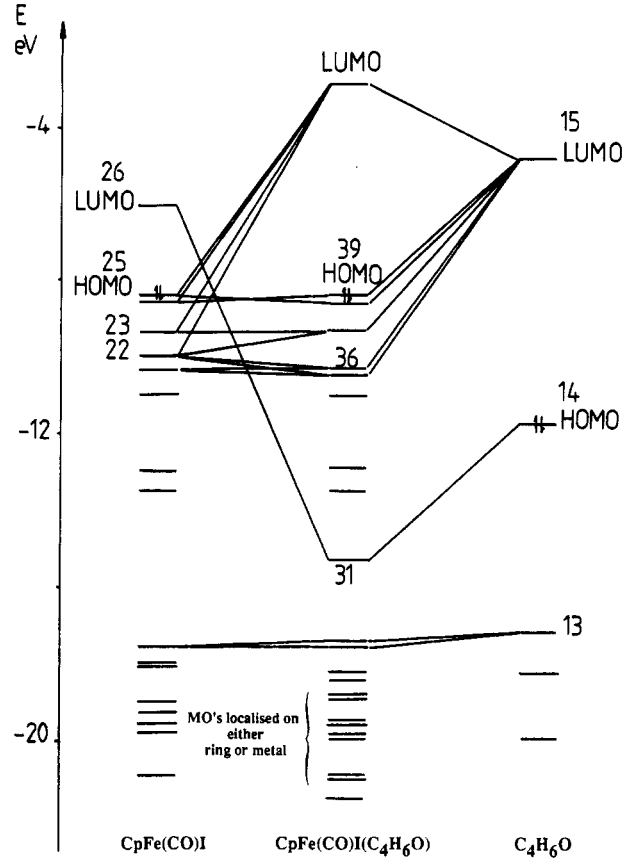

Figure 4. Fragment orbital correlation diagram for the formation of CpFeI(CO){=C(CH$_2$)$_3$O} (**4**) in geometry **4a** from the fragments CpFeI(CO) and {=C(CH$_2$)$_3$O}. Fragment orbital eigenvalues are taken from the Fock matrix of the complex.[23]

isomer for which the C(carbonyl)–Fe–C(carbene)–O dihedral angle is zero. In each case the energy zero is defined as that calculated for the experimentally observed orientation of each conformer (158.5° for **4a** and 356.5° for **4b**). Two curves are present because of the lack of flexibility inherent in the calculation. However, it is seen that the dihedral angles calculated for the maxima and minima correspond well, while the absolute energy correspondence is less good. This is because of the neglected relaxation effects (which would lower the real energy barrier).

In each case, a relatively large peak is associated with interference between the C(3)/C(13) methylene group and the iodide. The smaller peak in each case represents conflict between the same methylene and the cyclopentadienyl group. The oxygen atom α to the carbene does not interact strongly with either group as it rotates past.

Fenske–Hall Calculations. The Fenske–Hall quantum-chemical approach[10] gives a useful representation of the bonding in **4**. This is done by initially generating the frontier molecular orbitals of the CpFeI(CO) fragment and then examining their compatibility with those of the {=C(CH$_2$)$_3$O} ring using the axis system of Figure 2. A correlation of the two sets of fragment orbitals is presented in Figure 4.

The picture is relatively simple. There are just two MO's on the {=C(CH$_2$)$_3$O} ring fragment that are important in terms of interfragment interaction. These are the LUMO (MO 15) and the HOMO (MO 14). These orbitals are shown schematically in Figure 5.

The HOMO is the carbene lone pair. This orbital interacts effectively with the symmetric LUMO of the CpFeI(CO) fragment. This is the typical carbene–metal

(9) (a) Burkert, U.; Allinger, N. L. *Molecular Mechanics*; ACS Monograph 177; American Chemical Society: Washington, DC, 1982. (b) Boyd, D. B.; Kipowitz, K. B. *J. Chem. Educ.* **1982**, *59*, 269. (c) Allinger, N. L.; Tribble, M. T.; Miller, M. A.; Wertz, D. H. *J. Am. Chem. Soc.* **1971**, *93*, 1637. (d) Clark, T. *Computational Chemistry*; Wiley: New York, 1985.

(10) Hall, M. B.; Fenske, R. F. *Inorg. Chem.* **1972**, *11*, 768.

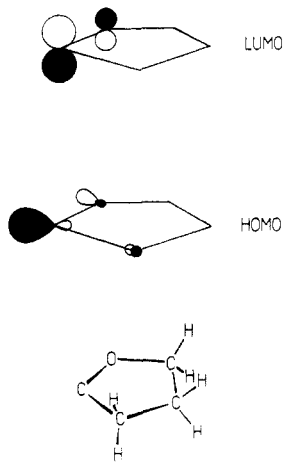

Figure 5. Schematic representations of the major interaction orbitals of the {=C(CH$_2$)$_3$O} fragment.

donor interaction. This single interaction accounts for 64% of the total interfragment Mulliken overlap population, with the occupancy of the HOMO of the {=C(CH$_2$)$_3$O} fragment decreasing from 2.00 to 1.34 on formation of **4**. The LUMO of the {=C(CH$_2$)$_3$O} ring possesses a symmetry compatible with that of MO's 22–25 of the CpFeI(CO) fragment. Back-bonding from the metal to the carbene therefore occurs through (15–22), (15–23), (15–24), and (15–25) orbital interactions. The resultant complex MO's are MO's 36–39. Molecular orbital 35 shows contributions from the fragment MO 15 ({=C(CH$_2$)$_3$O} fragment) and 21 (CpFeI(CO) fragment), but their mutual overlap is negligible.

Let us now consider the significance of the orientation of the {=C(CH$_2$)$_3$O} ring with respect to the CpFeI(CO) fragment in terms of perturbing the interfragment bonding. Experimentally, there are the two stable configurations **4a** and **4b**. With use of the convention of Figure 2, these refer to α = 0 and 162°. A series of calculations was performed on **4a** with the CpFeI(CO) fragment fixed and with the carbene ring fragment rotated through angles α about the Fe=C axis. As the orientation of the carbene ring is changed, there is no qualitative change in the correlation diagram of Figure 4. The interaction between fragment MO's 14 and 26 is clearly independent of the rotation angle α since it is directed along the rotation axis itself. However, the relative roles of the interactions (15–22), (15–23), (15–24), and (15–25) vary significantly. The variation in interfragment Mulliken overlap population totaled for these four interactions as a function of α is displayed in Figure 6. A detailed analysis of the overlap populations shows that, of the four contributory interactions, (15–22) is optimized close to α = 30° and (15–23) is most effective at α = 130°. These results are explained on examining amplitude contour maps for the frontier orbitals 22 and 23. These are shown in Figure 7.

Figure 7a shows MO 22 plotted in the xy plane and shows the compatibility of this MO with the carbene π orbital. However, a view of MO 22 in the yz plane (as seen by the incoming carbene ligand, Figure 7c) illustrates that the directionality of the orbital is slewed off the y axis. Hence, overlap between MO 22 and the LUMO of the ring fragment will be optimized if the {=C(CH$_2$)$_3$O} ring rotates through 30°. For MO 23, Figure 7b again shows compatibility with the carbene π orbital. Again, the orbital suffers from its skew off the y axis (Figure 7d), and this

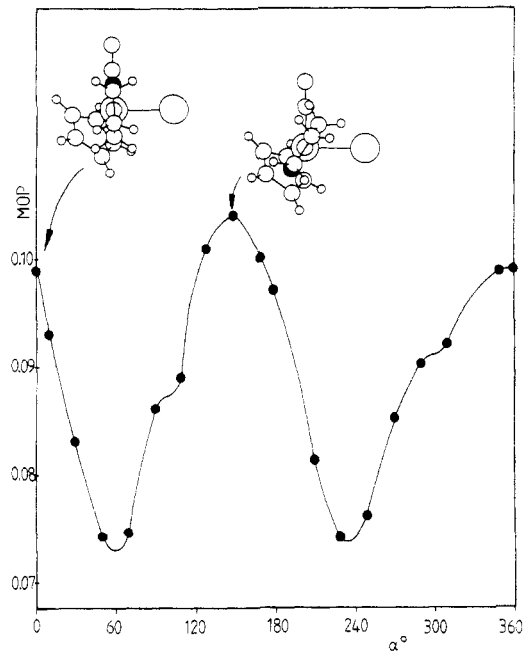

Figure 6. Summed Mulliken overlap populations for the interfragment interactions (22–15), (23–15), and (25–15) plotted as a function of the rotation angle α, defined in Figure 2. The inset sketches, viewed along the C$_{carbene}$–Fe axis, show the orientations of the {=C(CH$_2$)$_3$O} ring relative to the CpFeI(CO) fragment of the two maxima; the O atom of the ring fragment is colored black.

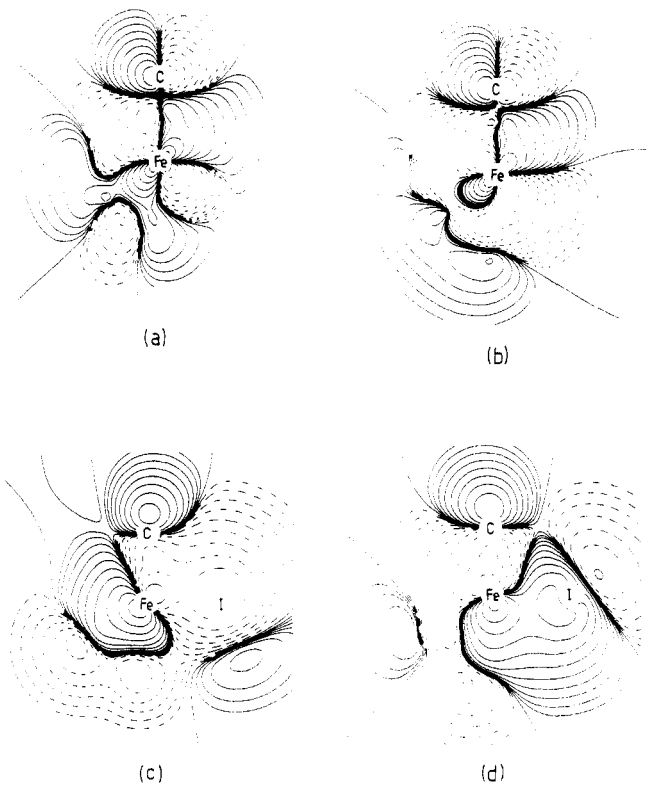

Figure 7. Amplitude contour plots for MO's 22 and 23 of the CpFeI(CO) fragment. Plots a and b show MO's 22 and 23, respectively, in the xy plane; plots c and d show MO's 22 and 23, respectively, in the yz plane at x = 0.5 Å.

feature will drive the {=C(CH$_2$)$_3$O} ring to twist through 130° in order to optimize orbital interaction. The interfragment overlaps for the two remaining combinations (15–24) and (15–25) exhibit a less dramatic effect upon α; nevertheless, the variation is significant and results in a shift of the net Mulliken overlap population maxima to

Scheme II

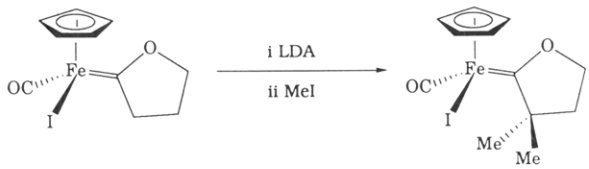

4 7

the points illustrated in Figure 6. It is gratifying to see that these final maxima correspond to $\alpha = 0$ and 150°; that is, there is good agreement with the experimentally determined {=C(CH$_2$)$_3$O} ring orientations. There is therefore an implication that electronic effects are indeed important in determining the stable conformations of the carbene fragment.

Finally, there is a small, but perhaps significant, secondary electronic effect that may also contribute toward the choice of ring orientation. As {=C(CH$_2$)$_3$O} rotates about the Fe=C axis, a finite overlap population develops between the carbene atom and the iodine atom. While the magnitude of this interaction is very small (≤0.02 electron), it is interesting that it is maximized for $\alpha = 0$ and 155°, close to the experimentally derived results.

Previous calculations suggest that the most favorable orientation of the carbene in the dicarbonyl cation [CpFe(=CR$_2$)(CO)$_2$]$^+$ is with the carbene symmetrically disposed in an upright fashion as in structures **5**.[11] This

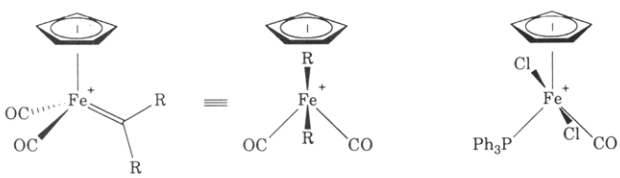

5 6

is the structure seen in the crystal structures of [CpFe(=CCl$_2$)(CO)$_2$]BCl$_4$[12] and [CpFe{=CH(SPh)}(CO)$_2$]PF$_6$,[13] for instance. The effect of asymmetry in the molecule as in [CpFe(=CF$_2$)(CO)(PPh$_3$)]BF$_4$ (**6**) is calculated[14] and observed[12] to force the carbene ligand to twist such that the most stable configuration is with the carbene ligand lying coplanar with the best π-acceptor ligand.

The situation is also related to that of acyl derivatives CpFe(COR)(CO)(PR$_3$), and a number of crystallographically characterized examples show the Fe–CO group lying approximately in the acyl plane with corresponding torsion angles very similar to those quoted for conformer **4b**.[15] We therefore see that the situation for CpFeI(CO){=C(CH$_2$)$_3$O} is related, except that experimentally we observe two stable conformations. One of the two stable conformers has the carbene twisted so that its plane lies parallel to the best π-acceptor, in this case carbonyl, while the situation for the second conformer is discussed above.

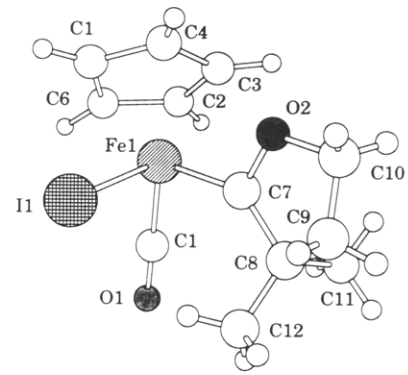

Figure 8. Structure of the complex CpFeI(CO){=CCMe$_2$(CH$_2$)$_2$O} (**7**).

Scheme III

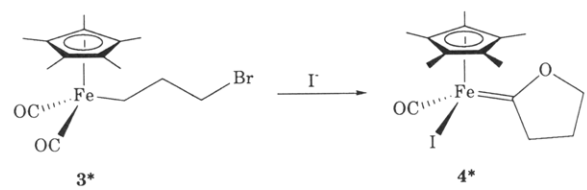

3* 4*

CpFeI(CO){=CCMe$_2$(CH$_2$)$_2$O} (7). One way to force the orientation of the carbene ring is to place substituents on the methylene group α to the carbene. Substituents here would be expected to interact sterically with the cyclopentadienyl ring. Two methyl substituents are introduced reasonably satisfactorily by reaction of **4** with excess lithium diisopropylamide (LDA) followed by MeI (Scheme II). The resulting compound CpFeI(CO)(=CCMe$_2$(CH$_2$)$_2$O} (**7**) is often contaminated with quantities of the monomethyl derivative CpFeI(CO){CCHMe(CH$_2$)$_2$O}, but this is separable by careful chromatography and recrystallization. This procedure is less satisfactory than the corresponding reaction of [CpFe(CO)(PPh$_3$){=C(CH$_2$)$_3$O}]$^+$ with NHPr$^i_2$, largely because that complex is cationic.[16]

The X-ray crystal structure of **7** is shown in Figure 8, and indeed, there is just a single isomer.

Within the limited accuracy of the structure, bond lengths have acceptable values. The CpFeI(CO) fragment is essentially conventional, but the cyclopentadienyl ligand is bonded in a slightly asymmetrical η^5 fashion with the iron atom at a perpendicular distance from the mean plane (rms deviation 0.022 Å) of 1.738 Å. The {=CCMe$_2$(CH$_2$)$_2$O} group is attached by a short, formal Fe=C bond of length 1.90 Å. The sense of the oxygen atom is syn with the Cp ring. The three basal ligands are mutually perpendicular within 5°. The {=CCMe$_2$(CH$_2$)$_2$O} ligand is bonded asymmetrically to the iron atom in the sense that the exocyclic angles at C(7) differ by more than 22°. This brings O(2) closer to the iron (2.74 Å) than C(8). This situation does not approach η^2 bonding, but the distortion does bring the oxygen atom O(2) quite close to the cyclopentadienyl ring (shortest C–C distances of 2.95 and 2.98 Å). The carbene ring is again in an envelope configuration with C(9) out of the plane defined by Fe–C(7)–O(2)–C(10)–C(8) by 30°. The orientation of the carbene ring

(11) Schilling, B. E. R.; Hoffmann, R.; Lichtenberger, D. L. *J. Am. Chem. Soc.* **1979**, *101*, 585.
(12) Crespi, A. M.; Shriver, D. F. *Organometallics* **1985**, *4*, 1830.
(13) Knors, C.; Kuo, G.-H.; Lauher, J. W.; Eigenbrot, C.; Helquist, P. *Organometallics* **1987**, *6*, 988.
(14) Schilling, B. E. R.; Hoffmann, R.; Faller, J. W. *J. Am. Chem. Soc.* **1979**, *101*, 592.
(15) For example: CpFe{C(=O)CH$_2$CH(OH)Ph}(CO)(PPh$_3$) (−169°) and CpFe{C(=O)CH$_2$CH(NHPh)Ph}(CO)(PPh$_3$) (−174°) (both from Liebeskind, L. S.; Welker, M. E.; Fengl, R. W. *J. Am. Chem. Soc.* **1986**, *108*, 6328) and CpFe{C(=O)CH$_2$CH(OH)Et}(CO)(PPh$_3$) (−169°) (Davies, S. G.; Dorder-Hedgecock, I. M.; Warner, P.; Jones, R. H.; Prout, K. *J. Organomet. Chem.* **1985**, *285*, 213).

(16) Curtis, J. C.; Davies, S. G. *J. Chem. Soc., Chem. Commun.* **1984**, 747.

parallels that in isomer **4a**. The torsion angle C(1)–Fe(1)–C(7)–O(2) is −170°. Clearly a rotamer of **7** corresponding to the rotamer **4b** is disallowed purely on steric grounds. This is in accord with conformational analyses for ligands bound to the $CpFe(CO)(PPh_3)$ unit.[17]

We recently found that the synthesis outlined in Scheme I is extendible to Cp* molybdenum and tungsten systems.[18] This is also true for iron. Thus, reaction of $[Cp^*Fe(CO)_2]^-$ with $Br(CH_2)_3Br$ gives $Cp^*Fe\{(CH_2)_3Br\}(CO)_2$ (**3***) (Scheme III). No attempt was made to isolate this species, but its IR spectrum is closely related to that of **3**. It reacts with LiI in a "one pot" reaction to form the new complex $Cp^*FeI(CO)\{=\overline{C(CH_2)_3O}\}$ (**4***), but in rather low yield. The problem here is that the insertion step with LiI requires some time at reflux, and the effect is that production of $Cp^*FeI(CO)_2$ competes rather effectively with carbene formation. The spectroscopic data for **4*** require little comment. We have not yet determined the orientation of the $\{=\overline{C(CH_2)_3O}\}$ ring.

Experimental Section

General Procedures. Infrared spectra were recorded with Perkin-Elmer 257 and 1710 (Fourier transform, linked to a Perkin-Elmer 4600 data station) instruments. Proton NMR spectra were recorded with Bruker WP-80SY (80 MHz), Perkin-Elmer R34 (220 MHz), Bruker AM-250 (250 MHz), and Bruker WH-400 (400 MHz) spectrometers. Carbon-13 NMR spectra were recorded on the Bruker AM-250 and WH-400 instruments. Mass spectra were recorded with a Kratos MS 25 spectrometer operating at low resolution using electron impact, chemical ionization (NH_3), and fast atom bombardment modes.

All reactions were carried out under dinitrogen or argon atmospheres with use of deoxygenated solvents dried with appropriate reagents (THF from Na/benzophenone and petroleum ether (bp 40–60 °C throughout) from $LiAlH_4$) or used as supplied. Alumina was Brockmann activity II throughout. The compounds $Br(CH_2)_3Br$ (Aldrich), $[CpFe(CO)_2]_2$,[19] $CpFe\{(CH_2)_3Br\}(CO)_2$,[7] and $[Cp^*Fe(CO)_2]_2$[20] were purchased or synthesized by literature procedures.

Synthesis of $CpFeI(CO)\{=\overline{C(CH_2)_3O}\}$ (4). A solution of $CpFe\{(CH_2)_3Br\}(CO)_2$ (**3**) was prepared in THF (100 cm^3) according to the literature procedure[7] starting from $[CpFe(CO)_2]_2$ (6.0 g, 16.9 mmol). Lithium iodide (30 g, 224 mmol) was added to the resulting mixture, and this solution was heated at reflux overnight. Solvent was removed from the resulting dark brown mixture and the resulting oil extracted into CH_2Cl_2. After filtration through Al_2O_3, the filtrate was chromatographed on Al_2O_3 (22 × 3 cm). The major product, brown $CpFeI(CO)\{=\overline{C(CH_2)_3O}\}$ (**4**), was eluted with petroleum ether/CH_2Cl_2 (3:1) (5.8 g, 49%). Generally, small quantities of $CpFeI(CO)_2$ precede the main product on the column. Analytical and spectroscopic data for **4** are as follows. Anal. Calcd for $C_{10}H_{11}FeIO_2$: C, 34.7; H, 3.2. Found: C, 34.8; H, 3.3. IR (ν_{CO}, THF): 1963 cm^{-1}. Mass spectrum: found m/e 346 (calcd for M^+ ($C_{10}H_{11}FeIO_2$) 346), 318 ($[M - CO]^+$). ^1H NMR (δ_H, $CDCl_3$): 4.98 (ddd, J = 6, 8, 9 Hz, 1 H, OCH_2), 4.88 (s, 5 H, Cp), 4.83 (m, 1 H, OCH_2), 4.08 (ddd, J = 6, 8, 19 Hz, 1 H, $Fe{=}CCH_2$), 3.72 (ddd, J = 8, 9, 19 Hz, 1 H, $Fe{=}CCH_2$), 2.00 (m, 2 H, central CH_2). ^{13}C NMR (δ_C, $CDCl_3$): 331.0 (Fe=C), 220.3 (CO), 86.2 (Cp), 83.4 (OCH_2), 60.2 ($Fe{=}C(CH_2)$), 22.2 (central CH_2).

Synthesis of $CpFeI(CO)\{=\overline{CCMe_2(CH_2)_2O}\}$ (7). A solution of lithium diisopropylamide (LDA); 15 cm^3, 0.2 M in hexane, 3.0 mmol) was added to a solution of $CpFeI(CO)\{=\overline{C(CH_2)_3O}\}$ (**4**; 0.35 g, 1 mmol) in THF (50 cm^3) at −78 °C with stirring. After 10 min, MeI (1.0 g, 7.0 mmol) was added to the resulting green solution and the solution was warmed to ambient temperature. After removal of solvent, the residue was extracted into CH_2Cl_2 and filtered through alumina. Chromatography on alumina (10 × 2 cm) gave a light brown band eluted with petroleum ether/CH_2Cl_2 that crystallized from petroleum ether/CH_2Cl_2 (2:1) as brown needles of $CpFeI(CO)(=\overline{CCMe_2CH_2CH_2O})$ (**7**; 0.062 g, 17%). This compound is sometimes contaminated with $CpFeI(CO)(=\overline{CCHMeCH_2CH_2O})$, which can be removed by further chromatography and recrystallization. The contamination is suggested by extra signals in the ^1H NMR spectrum along with those required for **7**, but the signal/noise ratio and signal overlaps prevent adequate characterization of this contaminant. Analytical and spectroscopic data for **7** are as follows. Anal. Calcd for $C_{12}H_{15}FeIO_2$: C, 38.5; H, 4.0. Found: C, 38.5; H, 4.3. IR (ν_{CO}, THF): 1948 cm^{-1}. Mass spectrum: found m/e 374 (calcd for M^+ ($C_{12}H_{15}FeIO_2$) 374), 346 ($[M - CO]^+$). ^1H NMR (δ_H, $CDCl_3$): 4.95 (dt, J = 10, 7 Hz, 1 H, OCH_2), 4.80 (s, 5 H, Cp), 4.81 (dt, J = 10, 8 Hz, 1 H, OCH_2), 1.87 (dd, J = 6, 8 Hz, 2 H, central CH_2), 1.57 (s, 3 H, Me), 1.35 (s, 3 H, Me). ^{13}C NMR (δ_C, $CDCl_3$): 345.0 (Fe=C), 221.0 (CO), 85.9 (Cp), 81.3 (OCH_2), 66.1 ($Fe{=}C(CMe_2)$), 36.9 (central CH_2), 27.3 (Me), 25.5 (Me).

Synthesis of $Cp^*FeI(CO)\{=\overline{C(CH_2)_3O}\}$ (4*). A solution of $[Cp^*Fe(CO)_2]_2$ (1.0 g, 2.0 mmol) in THF (50 cm^3) was treated with sodium–potassium alloy for 24 h to give a solution containing $K[Cp^*Fe(CO)_2]$. The solution was filtered through a glass frit and added dropwise (syringe pump) to a cooled (−20 °C) solution of $Br(CH_2)_3Br$ (2.5 g, 12.4 mmol) in THF (10 cm^3). After the mixture was warmed to ambient temperature and stirred for a further 1 h, the IR spectrum (ν_{CO} (THF) 1985s and 1929 cm^{-1}) indicated the presence of $Cp^*Fe\{(CH_2)_3Br\}(CO)_2$ (**3***). Lithium iodide (3.0 g, 22.4 mmol) was added to the resulting solution and the mixture heated at reflux for 3 days. The solvent was removed under reduced pressure; the residue was extracted into CH_2Cl_2 and the extract filtered thorugh Al_2O_3. Chromatography on Al_2O_3 with petroleum ether/CH_2Cl_2 (9:1) as eluent gave $Cp^*FeI(CO)_2$ (0.72 g, 48%) followed by brown microcrystalline $Cp^*FeI(CO)\{=\overline{C(CH_2)_3O}\}$ (**4***) (0.11 g, 7%). Analytical and spectroscopic data for **4*** are as follows. Anal. Calcd for $C_{15}H_{21}FeIO_2$: C, 43.3; H, 5.1. Found: C, 43.2; H, 5.0. IR (ν_{CO}, THF): 1937 cm^{-1}. Mass spectrum: found m/e 416 (calcd for M^+ ($C_{10}H_{11}FeIO_2$) 416), 388 ($[M - CO]^+$). ^1H NMR (δ_H, $CDCl_3$): 4.98 (ddd, J = 6, 8, 9 Hz, 1 H, OCH_2), 4.77 (ddd, J = 8, 8, 9 Hz, 1 H, OCH_2), 4.03 (ddd, J = 6, 8, 19 Hz, 1 H, $Fe{=}CCH_2$), 3.47 (ddd, J = 8, 8, 19 Hz, 1 H, $Fe{=}CCH_2$), 1.90 (m, 2 H, central CH_2), 1.82 (s, 15 H, Cp*). ^{13}C NMR (δ_C, $CDCl_3$): 326.2 (Fe=C), 222.1 (CO), 95.5 (C_5Me_5), 83.4 (OCH_2), 59.9 ($Fe{=}C(CH_2)$), 22.8 (central CH_2), 10.4 (C_5Me_5).

Molecular Mechanics Calculations. Energy calculations were carried out for each isomer **4a** and **4b** with use of a molecular mechanics method as embodied in the program MM2 as implemented on Chem3D Plus (Cambridge Scientific Computing Inc.). The molecule $CpFeI(CO)\{=\overline{C(CH_2)_3O}\}$ (**4**) was parameterized with C(3), C(4), and C(5) as type 1, C(2), C(6), and C(7) as type 2, C(1) as type 4, and O(1) and O(2) as type 6. This parameterization should account for a large part of the steric effect of the rotation, and the resulting plots are shown in Figure 3.

Fenske–Hall Calculations. Fenske–Hall calculations were carried out on the compound $CpFeI(CO)\{=\overline{C(CH_2)_3O}\}$ (**4**). A fixed geometry was used for the CpFeI(CO) fragment with bond parameters taken from the crystallographic data for **4**. The $\{=\overline{C(CH_2)_3O}\}$ fragment was positioned initially in the geometry of isomer **4b**. With the carbene atom fixed at 1.86 Å from the Fe atom, and with the Fe=C vector along the x axis, the $\{=\overline{C(CH_2)_3O}\}$ fragment was rotated α (α = 0–360°) about the x axis in the sense defined in Figure 2. Point calculations were performed for different values of α as described in the Results and Discussion. The non-hydrogen atoms of the $\{=\overline{C(CH_2)_3O}\}$ fragment were maintained planar throughout.

(17) (a) Blackburn, B. K.; Davies, S. G.; Sutton, K. H.; Whittaker, M. *Chem. Soc. Rev.* **1988**, *17*, 147. (b) Blackburn, B. K.; Davies, S. G.; Whittaker, M. In *Stereochemistry of Organometallic and Inorganic Compounds*; Bernal, I., Ed.; Elsevier: Amsterdam, 1989; Vol. 3, p 141.

(18) Bailey, N. A.; Dunn, D. A.; Foxcroft, C. N.; Harrison, G. R.; Winter, M. J.; Woodward, S. *J. Chem. Soc., Dalton Trans.* **1988**, 1449.

(19) *Organometallic Syntheses*; Eisch, J. J., King, R. B., Eds.; Academic Press: New York and London, 1965; Vol. 1.

(20) Catheline, D.; Astruc, D. *Organometallics* **1984**, *3*, 1094.

Table I. Summary of Crystal Data for Compounds 4 and 7

	4	7
formula	$C_{10}H_{11}FeIO_2$	$C_{12}H_{15}FeIO_2$
mol wt	345.95	374.00
cryst form	dark blocks	dark red blocks
cryst size, mm	0.05 × 0.08 × 0.25	0.6 × 0.2 × 0.3
cryst syst	triclinic	orthorhombic
space group	$P\bar{1}$	$Pbca$ (D_{2h}^{15}, No. 61)
a, Å	8.270 (10)	12.508 (21)
b, Å	8.312 (9)	12.53 (8)
c, Å	16.919 (17)	17.07 (4)
α, deg	98.66 (8)	90.000
β, deg	102.34 (8)	90.000
γ, deg	91.99 (9)	90.000
V, Å^3	1103 (2)	2674 (19)
D_c, g cm^{-3}	2.050	1.858
Z	4	8
radiation (λ, Å)	Mo Kα (0.71069)	Mo Kα (0.71069)
μ(Mo K$_\alpha$), cm^{-1}	40.21	33.96
F(000)	663.92	1455.84
diffractometer	Nicolet R3 four-circle	Nicolet R3 four-circle
temp	ambient	ambient
scan type	ω	ω
2θ range, deg	3.5–50	3.5–50
total no. of data	3946	2654
no. of unique obsd data	2875 ($\|F\|/\sigma(\|F\|) > 3.0$)	916 ($\|F\|/\sigma(\|F\|) > 3.0$)
R	0.0604	0.1241
R_w	0.0568	0.0937

Table II. Atom Coordinates (×10^4) and Temperature Factors (Å^2 × 10^3) for CpFeI(CO)[=C(CH$_2$)$_3$O] (4)

atom	x	y	z	U_{eq}[a]
I(1)	2355 (1)	1285 (1)	3659 (1)	57 (1)
I(2)	5670 (1)	1743 (1)	8654 (1)	54 (1)
Fe(1)	-848 (2)	823 (2)	3381 (1)	40 (1)
Fe(2)	5872 (2)	4818 (2)	8442 (1)	36 (1)
O(1)	-614 (12)	-2581 (11)	3527 (5)	74 (4)
O(2)	-1608 (11)	1422 (9)	1774 (4)	57 (3)
O(3)	2362 (10)	4977 (10)	8329 (5)	64 (3)
O(4)	4221 (11)	3994 (12)	6803 (4)	75 (4)
C(1)	-664 (14)	-1223 (14)	3470 (6)	44 (4)
C(2)	-955 (12)	410 (12)	2258 (6)	40 (4)
C(3)	-410 (15)	-993 (12)	1770 (7)	50 (4)
C(4)	-424 (16)	-473 (15)	931 (6)	58 (5)
C(5)	-1634 (18)	800 (16)	911 (7)	67 (5)
C(6)	-2933 (17)	2156 (17)	3213 (7)	70 (6)
C(7)	-3065 (17)	1005 (18)	3726 (9)	74 (6)
C(8)	-1847 (18)	1376 (18)	4435 (7)	70 (6)
C(9)	-900 (18)	2729 (19)	4351 (8)	75 (6)
C(10)	-1527 (17)	3243 (15)	3593 (9)	72 (6)
C(11)	3747 (13)	4901 (11)	8353 (6)	42 (4)
C(12)	5664 (13)	4255 (12)	7321 (6)	42 (4)
C(13)	6961 (15)	4004 (18)	6861 (7)	68 (5)
C(14)	6118 (21)	3568 (23)	5986 (9)	105 (8)
C(15)	4359 (20)	3608 (22)	5942 (7)	96 (7)
C(16)	8404 (16)	5544 (22)	8820 (10)	87 (7)
C(17)	7827 (19)	5277 (17)	9508 (8)	74 (6)
C(18)	6637 (18)	6276 (16)	9622 (7)	65 (5)
C(19)	6368 (17)	7229 (14)	9003 (8)	64 (5)
C(20)	7458 (20)	6818 (17)	8509 (8)	76 (6)

[a] The equivalent isotropic U_{eq} is defined as one-third of the trace of the orthogonalized U_{ij} tensor.

Table III. Bond Lengths (Å) and Bond Angles (deg) for CpFeI(CO)[=C(CH$_2$)$_3$O] (4)

(a) Bond Lengths

I(1)-Fe(1)	2.598 (2)	I(2)-Fe(2)	2.601 (2)
Fe(1)-C(1)	1.741 (12)	Fe(1)-C(2)	1.867 (10)
Fe(1)-C(6)	2.076 (14)	Fe(1)-C(7)	2.045 (15)
Fe(1)-C(8)	2.122 (14)	Fe(1)-C(9)	2.122 (14)
Fe(1)-C(10)	2.112 (13)	Fe(2)-C(11)	1.738 (11)
Fe(2)-C(12)	1.860 (10)	Fe(2)-C(16)	2.098 (11)
Fe(2)-C(17)	2.132 (13)	Fe(2)-C(18)	2.140 (15)
Fe(2)-C(19)	2.081 (11)	Fe(2)-C(20)	2.059 (15)
O(1)-C(1)	1.151 (15)	O(2)-C(2)	1.311 (13)
O(2)-C(5)	1.474 (14)	O(3)-C(11)	1.143 (14)
O(4)-C(12)	1.314 (12)	O(4)-C(15)	1.477 (15)
O(2)-C(3)	1.473 (15)	C(3)-C(4)	1.542 (17)
C(4)-C(5)	1.483 (20)	C(6)-C(7)	1.400 (21)
C(6)-C(10)	1.424 (18)	C(7)-C(8)	1.383 (17)
C(8)-C(9)	1.392 (22)	C(9)-C(10)	1.412 (20)
C(12)-C(13)	1.458 (18)	C(13)-C(14)	1.485 (18)
C(14)-C(15)	1.444 (24)	C(16)-C(17)	1.392 (24)
C(16)-C(20)	1.436 (23)	C(17)-C(18)	1.339 (21)
C(18)-C(19)	1.391 (19)	C(19)-C(20)	1.375 (22)

(b) Bond Angles

I(1)-Fe(1)-C(1)	90.2 (4)	I(1)-Fe(1)-C(2)	90.3 (3)
C(1)-Fe(1)-C(2)	92.0 (5)	Fe(1)-C(1)-O(1)	177.1 (11)
C(7)-C(8)-C(9)	107.0 (13)	C(8)-C(9)-C(10)	110.3 (11)
C(6)-C(7)-C(8)	109.3 (12)	C(6)-C(10)-C(9)	105.2 (12)
C(7)-C(6)-C(10)	108.1 (11)	C(2)-O(2)-C(5)	111.6 (9)
Fe(1)-C(2)-O(2)	121.3 (7)	Fe(1)-C(2)-C(3)	129.3 (8)
O(2)-C(2)-C(3)	109.3 (9)	C(2)-C(3)-C(4)	105.4 (9)
C(3)-C(4)-C(5)	101.4 (10)	O(2)-C(5)-C(4)	105.5 (9)
I(2)-Fe(2)-C(11)	90.7 (3)	I(2)-Fe(2)-C(12)	89.1 (3)
C(11)-Fe(2)-C(12)	93.1 (5)	Fe(2)-C(11)-O(3)	177.2 (10)
C(17)-C(18)-C(19)	108.9 (13)	C(18)-C(19)-C(20)	107.7 (12)
C(16)-C(17)-C(18)	110.3 (13)	C(16)-C(20)-C(19)	107.9 (13)
C(17)-C(16)-C(20)	105.1 (14)	C(12)-O(4)-C(15)	113.2 (10)
Fe(2)-C(12)-O(4)	122.7 (9)	Fe(2)-C(12)-C(13)	128.9 (7)
O(4)-C(12)-C(13)	108.4 (9)	C(12)-C(13)-C(14)	106.8 (11)
C(13)-C(14)-C(15)	107.1 (13)	O(4)-C(15)-C(14)	104.4 (10)

Table IV. Atom Coordinates (×10^4) and Temperature Factors (Å^2 × 10^3) for CpFeI(CO)[CCMe$_2$(CH$_2$)$_2$O] (7)

atom	x	y	z	U_{eq}[a]
I(1)	-4298 (2)	-5479 (2)	-1766 (2)	65 (1)*
Fe(1)	-3113 (3)	-3820 (4)	-2078 (3)	40 (2)*
O(1)	-1274 (19)	-4504 (20)	-1213 (15)	85 (8)
O(2)	-4649 (15)	-2504 (16)	-1462 (12)	52 (6)
C(1)	-2032 (27)	-4247 (24)	-1530 (21)	63 (11)
C(2)	-2168 (26)	-2968 (23)	-2842 (19)	60 (11)
C(3)	-3106 (27)	-2437 (25)	-2766 (19)	63 (10)
C(4)	-3915 (26)	-3138 (24)	-3057 (20)	67 (11)
C(5)	-3384 (26)	-4088 (25)	-3321 (21)	65 (11)
C(6)	-2279 (25)	-3970 (23)	-3130 (19)	61 (10)
C(7)	-3814 (23)	-3111 (22)	-1237 (20)	45 (9)
C(8)	-3636 (24)	-2986 (23)	-383 (20)	48 (9)
C(9)	-4766 (28)	-2537 (30)	-125 (23)	82 (13)
C(10)	-5202 (25)	-1931 (22)	-797 (18)	55 (9)
C(11)	-2807 (24)	-2122 (23)	-298 (20)	73 (12)
C(12)	-3374 (26)	-3974 (22)	44 (19)	70 (11)

[a] Values marked with an asterisk are equivalent isotropic U_{eq} values, defined as one-third of the trace of the orthogonalized U_{ij} tensor.

The Fenske–Hall calculations employed single-ζ Slater functions for the 1s and 2s functions of C and O. The exponents were obtained by curve-fitting the double-ζ functions of Clementi[21] while maintaining orthogonal functions. The double-ζ functions were used directly for the 2p orbitals. An exponent of 1.16 was used for H. The Fe 1s–3d functions were taken from the results of Richardson[22] and were single-ζ, except for the 3d function, which was double-ζ, and were chosen for the +1 oxidation state. Both 4s and 4d exponents for Fe were 2.00. Exponents for iodine were taken from the results of Richardson and augmented with 5s and 5p functions.

X-ray Crystal Structure Analyses. The X-ray data are summarized in Table I.

CpFeI(CO)[=C(CH$_2$)$_3$O] (4). The unit cell dimensions were derived from the setting angles of 16 reflections in the range 5° ≤ 2θ ≤ 22°. Intensity data were collected over half the sphere

(21) (a) Clementi, E. *J. Chem. Phys.* **1964**, *40*, 1944. (b) Clementi, E.; Raimondi, D. L.; Reinhardt, W. P. *J. Chem. Phys.* **1967**, *47*, 1300.

(22) Richardson, J. W.; Nieuwpoort, W. C.; Powell, R. R.; Edgell, W. F. *J. Chem. Phys.* **1962**, *36*, 1057.

(23) Kostic, N. M.; Fenske, R. F. *Organometallics* **1982**, *1*, 974.

Table V. Bond Lengths (Å) and Bond Angles (deg) for CpFeI(CO){=CCMe$_2$(CH$_2$)$_2$O} (7)

(a) Bond Lengths

I(1)-Fe(1)	2.608 (12)	Fe(1)-C(1)	1.729 (35)
Fe(1)-C(2)	2.058 (33)	Fe(1)-C(3)	2.092 (33)
Fe(1)-C(4)	2.128 (35)	Fe(1)-C(5)	2.173 (36)
Fe(1)-C(6)	2.084 (34)	Fe(1)-C(7)	1.903 (33)
O(1)-C(1)	1.138 (42)	O(2)-C(7)	1.349 (35)
O(2)-C(10)	1.509 (37)	C(2)-C(3)	1.354 (46)
C(2)-C(6)	1.355 (42)	C(3)-C(4)	1.429 (46)
C(4)-C(5)	1.435 (45)	C(5)-C(6)	1.428 (45)
C(7)-C(8)	1.483 (49)	C(8)-C(9)	1.584 (47)
C(8)-C(11)	1.506 (42)	C(8)-C(12)	1.472 (42)
C(9)-C(10)	1.480 (49)		

(b) Bond Angles

I(1)-Fe(1)-C(1)	95.0 (11)	I(1)-Fe(1)-C(7)	87.4 (9)
C(1)-Fe(1)-C(7)	95.5 (15)	Fe(1)-C(1)-O(1)	175.0 (32)
C(3)-C(2)-C(6)	113.6 (30)	C(2)-C(3)-C(4)	106.2 (28)
C(3)-C(4)-C(5)	106.9 (28)	C(4)-C(5)-C(6)	106.9 (27)
C(2)-C(6)-C(5)	106.1 (27)	C(7)-O(2)-C(10)	114.1 (23)
Fe(1)-C(7)-O(2)	113.9 (23)	Fe(1)-C(7)-C(8)	136.2 (22)
O(2)-C(7)-C(8)	109.7 (25)	C(7)-C(8)-C(9)	100.2 (25)
C(7)-C(8)-C(11)	105.9 (26)	C(9)-C(8)-C(11)	109.4 (25)
C(7)-C(8)-C(12)	115.5 (26)	C(9)-C(8)-C(12)	111.1 (27)
C(11)-C(8)-C(12)	113.8 (27)	C(8)-C(9)-C(10)	107.2 (29)
O(2)-C(10)-C(9)	99.8 (24)		

and corrected for Lorentz and polarization effects. Two check reflections monitored once every 100 measurements showed no evidence of decay. No absorption correction was necessary because of the small size of the crystal. The structure was solved by Patterson and difference Fourier methods and refined by cascade blocked-diagonal least squares (254 refined parameters) with use of the SHELXTL suite of programs on a NOVA 3 computer. The weighting scheme was $w = [\sigma^2(|F|) + gF^2]^{-1}$ with $g = 0.0011$. Hydrogen atoms were inserted at calculated positions and constrained to ride on their neighboring heavy atoms. Their thermal parameters were fixed at 1.2 times those for the neighboring heavy atoms. The structures are illustrated in Figure 1; details are given in Tables II and III and in the supplementary material (hydrogen atom positional parameters, anisotropic thermal vibrational parameters with esd's, observed structure amplitudes and calculated structure factors).

CpFeI(CO){=CCMe$_2$(CH$_2$)$_2$O} (7). The 916 observed reflections were corrected for Lorentz effects, for polarization effects, and for absorption on the basis of azimuthal scans. The structure was solved by standard Patterson and Fourier techniques and refined by blocked-cascade least-squares methods to a final $R = 0.1241$, with allowance for the anisotropic thermal vibration of iron and iodine only. Complex scattering factors were taken from the program package SHELXTL (as implemented on the NOVA 3 computer) used for the refinement. Hydrogen atoms were placed in calculated positions with isotropic thermal parameters linked to those of the supporting atom. The weighting scheme was $w = [\sigma^2(|F|) + gF^2]^{-1}$ with $g = 0.0005$. The structure is illustrated in Figure 8; details are given in Tables IV and V and in the supplementary material (hydrogen atom positional parameters, anisotropic thermal vibrational parameters with esd's, observed structure amplitudes and calculated structure factors).

Acknowledgment. We are pleased to acknowledge the SERC and the Royal Society for financial support. The Royal Society is also acknowledged for a 1983 Research Fellowship (to C.E.H.), and the SERC is also acknowledged for a Research Studentship (to C.R.). We thank the reviewers for perceptive comments.

Supplementary Material Available: Tables of hydrogen atom coordinates and anisotropic thermal parameters for 4 and 7 (3 pages); tables of observed and calculated structure factors (23 pages). Ordering information is given on any current masthead page.

Notes

Carbon–Carbon Bond Formation by Coupling of Two Phenylethynyl Ligands in an Organolanthanide System

William J. Evans,* Roy A. Keyer, and Joseph W. Ziller

Department of Chemistry, University of California, Irvine, Irvine, California 92717

Received March 8, 1990

Summary: $[(C_5Me_5)_2Sm]_2(\mu\text{-}\eta^2\text{:}\eta^2\text{-}PhC_4Ph)$, a crystallographically characterized complex that previously has been isolated from the reaction of $(C_5Me_5)_2Sm(THF)_2$ with PhC≡CC≡CPh, can be obtained from organosamarium precursors derived from PhC≡CH. $[(C_5Me_5)_2Sm]_2(\mu\text{-}\eta^2\text{:}\eta^2\text{-}PhC_4Ph)$ is formed from the reaction of $[(C_5Me_5)_2Sm(\mu\text{-}H)]_2$ with PhC≡CH, from the thermolysis of $(C_5Me_5)_2Sm(C{\equiv}CPh)(THF)$ at 80–145 °C, from the reaction of $(C_5Me_5)_2Sm$ with PhC≡CH, and from the reaction of $(C_5Me_5)_2Sm[CH(SiMe_3)_2]$ with PhC≡CH, a reaction that has been reported to form $[(C_5Me_5)_2Sm(\mu\text{-}C{\equiv}CPh)]_2$.

Ligand-coupling reactions constitute one of the important classes of metal-mediated transformations in organometallic chemistry.[1] For example, the formation of a new bond between two reductively eliminated ligands plays an important role in many metal-based catalytic cycles. Comparable processes are not common in organolanthanide chemistry.[2-6] For monometallic complexes, simple reductive elimination is not possible since none of

(1) Collman, J. P.; Hegedus, L. S.; Norton, J. R.; Finke, R. G. *Principles and Applications of Organotransition Metal Chemistry*, 2nd ed.; University Science Books: Mill Valley, CA, 1987.
(2) Forsberg, J. H.; Moeller, T. In *Gmelin Handbook of Inorganic Chemistry*, 8th ed.; Moeller, T., Kruerke, U., Schleitzer-Rust, E., Eds.; Springer-Verlag: Berlin, 1983; Part D6, pp 137-282.
(3) Marks, T. J.; Ernst, R. D. In *Comprehensive Organometallic Chemistry*; Wilkinson, G., Stone, F. G. A., Abel, E. W., Eds.; Pergamon Press: Oxford, England, 1982; Chapter 21.
(4) Schumann, H.; Genthe, W. In *Handbook on the Physics and Chemistry of Rare Earths*; Gschneidner, K. A., Jr., Eyring, L., Eds.; Elsevier: Amsterdam, 1985; Vol. 7, Chapter 53, and references therein.
(5) Evans, W. J. *Adv. Organomet. Chem.* **1985**, *24*, 131-177.
(6) Evans, W. J. *Polyhedron* **1987**, *6*, 803-835.

0276-7333/90/2309-2628$02.50/0